JASA ARTICLE

Physical effects of sound exposure from underwater explosions on Pacific sardines (*Sardinops sagax*)[a)]

Peter H. Dahl,[1,b)] A. Keith Jenkins,[2] Brandon Casper,[3] Sarah E. Kotecki,[2] Victoria Bowman,[2] Christiana Boerger,[2] David R. Dall'Osto,[1] Matthew A. Babina,[3] and Arthur N. Popper[4,c)]

[1]*University of Washington, Seattle, Washington 98195, USA*

[2]*Naval Information Warfare Center Pacific, San Diego, California 92110, USA*

[3]*Naval Submarine Medical Research Laboratory, Groton, Connecticut 06349, USA*

[4]*University of Maryland, College Park, Maryland 20742, USA*

ABSTRACT:

Explosions from activities such as construction, demolition, and military activities are increasingly encountered in the underwater soundscape. However, there are few scientifically rigorous data on the effects of underwater explosions on aquatic animals, including fishes. Thus, there is a need for data on potential effects on fishes collected simultaneously with data on the received signal characteristics that result in those effects. To better understand potential physical effects on fishes, Pacific sardines (*Sardinops sagax*) were placed in cages at mid-depth at distances of 18 to 246 m from a single mid-depth detonation of C4 explosive (4.66 kg net explosive weight). The experimental site was located in the coastal ocean with a consistent depth of approximately 19.5 m. Following exposure, potential correlations between blast acoustics and observed physical effects were examined. Acoustic metrics were calculated as a function of range, including peak pressure, sound exposure level, and integrated pressure over time. Primary effects related to exposure were damage to the swim bladder and kidney. Interestingly, the relative frequency of these two injuries displayed a non-monotonic dependence with range from the explosion in relatively shallow water. A plausible explanation connecting swim bladder expansion with negative pressure as influenced by bottom reflection is proposed. https://doi.org/10.1121/10.0001064

(Received 23 December 2019; revised 22 February 2020; accepted 22 March 2020; published online 20 April 2020)

[Editor: James F. Lynch] Pages: 2383–2395

I. INTRODUCTION

There is growing concern about the potential effects of anthropogenic sound on aquatic life (e.g., see papers in Popper and Hawkins, 2016). While there have been studies assessing these potential effects on marine mammals (reviewed in NMFS, 2018; Southall *et al.*, 2019), there have been fewer studies on fishes (reviewed in Carroll *et al.*, 2017; Popper and Hawkins, 2019; Popper *et al.*, 2019; Putland *et al.*, 2019). Moreover, fish studies have focused on effects of sounds produced by vessels, sonars, pile driving (e.g., used in wind farm construction), and seismic air guns (Hawkins and Popper, 2018; Popper and Hawkins, 2019; Popper *et al.*, 2019). In contrast, there have been few studies directed at potential effects of the sounds from underwater explosions used in construction, demolition, military activities, etc. At the same time, the need for more detailed analyses required for protected species drives the interest in having additional data on the effects of high-energy sound that can result from such explosive activities.

The few studies on effects of explosions on fishes are limited in the information they provide because they were, for the most part, done in restricted acoustic environments (i.e., not open water), often with few controls, and/or with limited procedures for post-exposure necropsy (Coker and Hollis, 1950; Hubbs and Rechnitzer, 1952; Gaspin, 1975; Linton *et al.*, 1985; Yelverton *et al.*, 1991; Goertner *et al.*, 1994). More comprehensive studies were done by Govoni *et al.* (2003) and Govoni *et al.* (2008) on juvenile and larval fishes (length $\sim$ 20 mm). With these size limitations in mind, Govoni and colleagues found that integrated pressure over time interval corresponding to 95% of the energy, or pressure impulse (dimension Pa s), to be the most relevant metric for describing dose-response.

In contrast to earlier work, the study reported here examines the effects of exposure to an explosion on caged adult fish located at different distances from the source using ample controls and detailed necropsy procedures. Of fundamental importance is that this study was done in an open-water location, which is more representative of marine fish habitat. Open water is defined here as a body of water for which the range (length) and width scales are effectively infinite, and in which boundary reflections originate primarily from the seabed and the sea surface.

The initial hypothesis for this study was that effects would decrease with increased distance from the source (i.e., as the acoustic dose in terms of pressure or energy level decreased), as suggested in recent pile driving studies (e.g.,

[a)]This paper submitted as part of the Special Issue of JASA on Effects of Noise on Aquatic Life.

[b)]Electronic mail: dahl@apl.washington.edu

[c)]ORCID: 0000-0002-0312-7125.

Casper *et al.*, 2012; Halvorsen *et al.*, 2012a; Halvorsen *et al.*, 2012b). However, while this pattern was observed for fish located close to the explosion, this was not the case at greater distances. At such distances, effects associated with the underwater waveguide, such as reflection from the seabed, are postulated to play a role in observations of increased rates of injury at some locations farther from the source at this site.

II. METHODS

A. Study overview

The general approach in the study was to transport animals out to the open-water test site, place them in instrumented test cages located at different distances from the source, lower them to mid-water depth, and expose them to a single explosion. Following exposure, the cages were brought to the surface, where the fish were removed from the cages, sacrificed with an overdose of anesthetic, chilled, and then transported to a shore-based laboratory where they were necropsied on the same day. Control fish were exposed to identical conditions as the experimental animals other than the explosion. Data from the sensors on the cages enabled a complete analysis of the acoustic environment to which the fish were exposed. This procedure was repeated on four trial days in October 2018, with a single explosion each day.

B. Experimental species

The study used the Pacific sardine (*Sardinops sagax*), a pelagic species with a physostomous swim bladder commonly found in the waters off San Diego, CA, at depths that include those used in this study (Miller and Lee, 1972). Physostomous swim bladders have a direct connection to the gut (via the pneumatic duct) allowing for easy transfer of gasses in and out of the swim bladder via "gulping" or "burping" of air.

The fish used in the study were obtained from a commercial bait dock in San Diego Bay and held for seven months at the National Marine Fisheries Service's Southwest Fisheries Center in La Jolla, CA. Fish were then removed from their holding tanks and transported to Naval Base Point Loma (San Diego), where they were kept in 1.2 m deep seawater pens at the mouth of the San Diego Bay for a minimum of two weeks prior to being used in the study. Fish were fed pellet food and cared for daily. At the time of the study, fish had a mean standard length of 166 mm [standard deviation (SD) 9 mm] and mean weight of 62 g (SD 11 g).

All procedures were approved by the Naval Information Warfare Center Pacific Institutional Animal Care and Use Committee (IACUC, protocol 131–2018), and the Navy Bureau of Medicine and Surgery. The study followed all relevant U.S. Department of Defense guidelines for the care and use of laboratory animals.

C. Explosive source

The explosive source for each trial consisted of 3.4 kg of C4 explosive, which corresponds to 4.66 kg of trinitrotoluene (TNT) using a TNT-equivalent coefficient of 1.37. Detonations occurred at a depth of 10.5 m (±0.5 m), approximately mid-column at the site, to avoid immediate interaction of the explosion with the bottom. The detonations were conducted by Navy explosive ordnance demolition personnel in accordance with the U.S. Navy's Hawaii-SOCAL Environmental Impact Statement[1] and associated permits.

D. Experimental site

All trials occurred within the U.S. Navy's Silver Strand Training Complex, an area approximately 5 km offshore from San Diego. All instrumented experimental cages and other acoustic sensors were located along a line parallel to the shoreline over which the average water depth was 19.5 m, with little bathymetric variation over the transect (about 250 m long). The seabed within the immediate area is largely composed of unconsolidated, sandy sediments.

E. Fish cages, basic measurement geometry and acoustic instrumentation

The approximately 0.35 m^3 cylindrical cages were covered with 1.5 cm knotless polyester mesh netting and suspended within a frame made from polyvinyl chloride (PVC) tubing (Fig. 1). The cages were suspended close to mid-water using a 9.2 m line with an approximately 20 kg weight to anchor the station to the seabed, which put the cage center at a depth of 10.5 m (±0.5 m). A closed cell foam float was tied at the top of the cage to ensure that it maintained correct orientation. From this subsurface float, another line was run to the surface and attached to either marker buoys (control cages) or inflatable rafts with the acoustic monitoring system

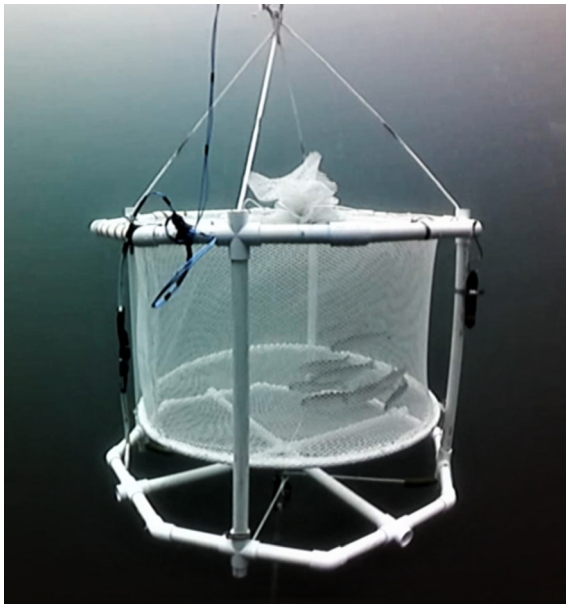

FIG. 1. (Color online) Underwater photo of one of the cages taken with a ROV prior to exposure to the explosion. Details of the cage, instrumentation, and its suspension are discussed in the text. A depth sensor is shown on the right of the cage and a pair of blast probes on the left. Pacific sardines can be seen schooling in the cage.

https://doi.org/10.1121/10.0001064

(discussed in detail in the next paragraph). All cages beyond 50 m from the blast were equipped with depth sensors. Depth sensors could not be placed closer than about 50 m without being damaged; however, depth-consistency over the four instrumented cages gives confidence in assigning the depth for such case.

The four closest experimental cages were each instrumented with two, non-directional, tourmaline blast sensors (PCB W138A01, PCB Piezotronics, Depew, NY) with nominal sensitivity of 0.73 mV/kPa, equivalent to a received sensitivity of −243 dB re V/μPa. The two sensors (for redundancy) were wired to custom-designed recording and transmitting units housed in small inflatable rafts situated above each cage (see Fig. 2), which recorded the acoustic data at a 2-MHz sampling rate. Data from all four rafts were time-synchronized with a Global Positioning System (GPS) and recording was started remotely by a computer base station located on one of the monitoring boats.

The acoustic field at the farthest (or 5th) cage was measured by placing a nine-element vertical line array (VLA) as close as possible to the cage (Fig. 2). Acoustic data from the nine VLA elements (ITC 1042 non-directional hydrophone, nominal sensitivity of −206 dB re V/μPa, Gavial ITC, Santa Barbara, CA) were coherently recorded at a 0.5-MHz sampling rate. The VLA elements were separated by 2 m, and data from the VLA hydrophone at depth most closely matching the cage depth was taken as a measure of the acoustic field at this far range.

F. Explosion exposure paradigm

Experimental procedures were refined and preliminary fish cage ranges from the explosion were established during a pilot trial in September 2018 (data from that trial are not used in the results reported here). This established a protocol that was then followed during each of the four experimental trials.

On the morning of each of the four trials, approximately 80–90 fish were transferred by dip-net to three cylindrical holding tanks (height 1.5 m, diameter 0.7 m) located on the R/V *Ecos*, a 12.2-m-long Navy research vessel. Transport to the offshore research site took approximately 45 min, during which time the holding tanks were continuously aerated. In addition, fresh seawater was introduced to the holding tanks each time the vessel stationed to deploy fish cages or instrumentation. Dissolved oxygen levels were monitored at regular intervals and airflow was increased when levels dropped below 100%.

Upon arrival at each designated cage location, a cage (Fig. 1) was lowered halfway into the water. In most cases, ten fish were dip-netted into the cage. The cage was closed and slowly lowered (over a period of about 2 min) to the experimental depth. In a few instances, a cage received 9 or 11 fish, and this numerical variation was incorporated into subsequent statistical analysis. Fish displaying abnormal swimming in the transport containers were not used for the study.

The first two cages (controls) were deployed on the test range at the same depth as exposure cages. Once the control cages were positioned, the vessel stationed the five test cages along a 250-m-long transect (Fig. 2) originating from the detonation point. Over the four days of trials, 20 test cages were placed at distances ranging from 18 to 246 m. Once the test cages were in position, the vessel returned to the control cages, lifted them to the surface, and retrieved the fish. Control fish were treated identically to experimental fish other than for exposure to the explosions and were in the water for approximately the same duration (about 3 h) as the experimental fish.

After each test and control cage was positioned at depth, it was inspected with a remotely operated vehicle (ROV) operated from a small boat to ensure that the cage had deployed properly and that the fish were actively swimming (Fig. 1). Another small boat used GPS to get an accurate estimate of test cage position by stationing directly over the cage, and thus could determine distance from the explosion. This determination was critical because it was not possible in the open-water conditions to position a cage in a precise, pre-established location using the deployment procedure.

Concurrently with the deployment of cages, a U.S. Navy Explosive Ordnance Disposal (EOD) dive team

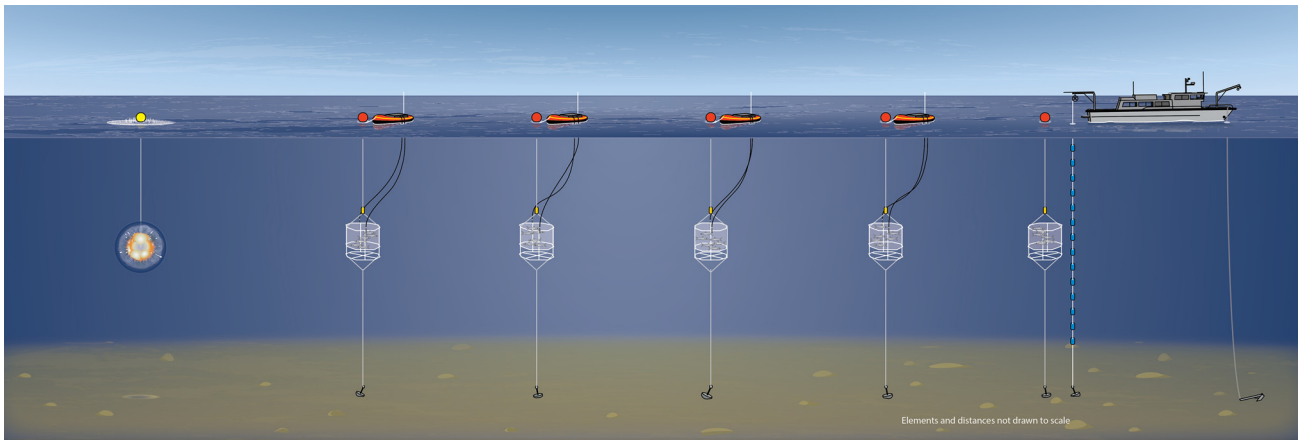

FIG. 2. (Color online) Basic geometry (not to scale) for each explosive trial (see text for additional information). The explosion is to the left. Five cages are deployed midwater out to maximum range of approximately 250 m from the source. Note the tourmaline blast sensors on the four cages closest to the source. These are attached by cable to the raft at the surface (red). The VLA was stationed adjacent to the farthest cage.

prepared the explosive charge. Once all fish cages were properly placed, the EOD dive team set the explosives at the predetermined location (with known GPS coordinates) and depth (10.5 m). Upon confirmation that all systems were recording and that a required mitigation zone around the blast site was clear of marine mammals, the EOD team began a countdown and the charge was detonated.

Approximately 15 min post-detonation (depending upon clearance from the EOD dive team), the R/V *Ecos* began recovery of the test cages. These were recovered in the same order they were deployed in order to maintain the same approximate time in the water (2 h 50 min ±20 min).

Immediately upon recovery of a cage, all live fish were euthanized by placing them in a solution of buffered anesthetic (MS-222, tricaine methanesulfonate) for approximately ten minutes beyond the last observed opercular movement (i.e., respiration). The fish were then removed from the anesthetic solution and immediately placed in plastic bags labeled to indicate the treatment (i.e., distance to the explosion or control). The few (eight) fish that were dead when brought to the surface in the cages were treated similarly except that they were not placed in the anesthetic and they were stored in separate bags from the euthanized fish. All bags were wrapped in bubble wrap or towels to prevent localized freezing of tissues when they were placed on ice packs. In addition, any animals that were transported to the test site but not deployed in exposure or control cages were euthanized after cages were deployed and subjected to the same storage procedures as used for the other fish. These fish were examined to inform any potential effects that resulted from handling or husbandry methods during initial dip netting and transportation to the test site (e.g., external abrasions).

G. Fish preparation and necropsy

Once the boat returned to shore, the chilled euthanized animals were immediately moved to the laboratory. Using a pre-determined randomization sequence, fish were taken from different bags (representing different treatments) for necropsy. Each fish received a unique identification number and was weighed, measured, and given to one of the individuals performing necropsies who were blind to the treatment of the fish.

Necropsy procedures were adapted from past studies examining the effects of impulsive anthropogenic sound on fishes (e.g., Casper *et al.*, 2012; Halvorsen *et al.*, 2012a; Halvorsen *et al.*, 2012b; Popper *et al.*, 2016). Dissection procedures were standardized among individuals performing necropsies and identification of natural variations in organs and tissue (e.g., color, size, and placement) was established by observing the baseline anatomy of Pacific sardines.

When given a fish, the investigator performing the necropsy first examined the exterior of the animal and noted any damage. They then opened the fish by making a ventral midline incision starting at the vent (cloaca) and moving forward to the pectoral girdle. Both sides of the cut were carefully pinned apart to reveal the internal organs. Using a blunt probe, the organs and tissues were inspected for any evidence of injury (see Table I for organs and tissues examined).

Each investigator made note of injuries or other observations (including any on tissue not on the observation list) using a tracking sheet. Photographs were taken of suspected injuries. Examination of each fish took 10–20 min, depending on the extent of damage. Once necropsy was completed, the tracking sheet was given to a data handler who entered the findings into a database. A second person later reviewed each entry for accuracy.

III. RESULTS

All but 8 of the 209 experimental fish were retrieved alive after exposure to the explosion. Four of the mortalities were at the closest cage (18 m). Note that since live fish were euthanized shortly after they were brought to the surface, it is not possible to know whether they would have

TABLE I. Summary of effects data. Data in columns 2, 3, and 4 rounded to one decimal. See text for explanations of each column. Bold injuries show statistical significance.

1 Injury	2 Pooled control rate (%)	3 Pooled injury rate (%)	4 SD (+/−)	5 *p*-value homogeneity with range	6 *p*-value injury significance
Spleen hematoma	0	0	-	-	No injury
Spleen hemorrhage	0.0	0.0	-	-	No injury
Body muscle hematoma	0.0	1.9	0.9	0.667	0.384
Pyloric caeca hemorrhage	1.4	3.0	2.0	0.073	0.389
Hepatic hemorrhage	0.0	2.9	1.2	0.424	0.197
Gall bladder damage	0.0	0.5	0.5	0.624	0.484
Swim bladder hematoma	0.0	3.3	1.0	0.175	0.144
Burst capillaries	0.0	3.3	1.2	0.030	-[a]
Fat hematoma	1.0	48.8	3.5	0.394	<0.001
Reproductive blood vessel rupture	0.0	15.8	2.5	0.017	<0.001[b]
Swim bladder rupture	0.0	19.6	2.7	0.001	<0.001
Kidney rupture	0.0	25.4	3.0	0.010	<0.001

[a]Injury rate shows statistical significance ($p < 0.01$) only when comparing the fish nearest the source to the controls [see Fig. 4(a)].
[b]Observation of this injury may not be possible in instances of severely ruptured swim bladder.

https://doi.org/10.1121/10.0001064

succumbed to internal injuries at any time following exposure. No mortalities were observed in control fish.

The ROV videos recorded prior to the detonation showed that most fish were schooling (i.e., swimming closely together in the same circular direction, see Fig. 1) and none were dead. Only about 4% were not schooling or were swimming into the top or sides of the cage netting.

A. Physical effects

1. External effects

Each fish was examined externally to determine if exposure to the explosions produced physical damage including bleeding and abrasions to the eyes, gills, inside of mouth, fins, and external body wall. No differences in type or number of injuries were seen between experimental animals and control animals (0.2 being the minimum p-value for the hypothesis of no observed difference for the 13 itemized external injuries.) Thus, it is inferred that the external injuries were the result of handling or could have occurred while the fish were being held in the seawater pens prior to use.

2. Internal effects

Initially, injury assessments were based on the list of 18 possible internal injuries identified in the aforementioned studies. However, not all of the 18 possible internal injuries were found in the current study (e.g., intestinal hematoma and hemorrhage) and were therefore eliminated from consideration in the analysis. In addition, a previously unreported injury, reproductive blood vessel rupture, was noted during the current study and added to those analyzed. Therefore, a total of 12 internal injuries were found in the current study in one or more animals (see Table I).

The cumulative results from the set of 12 internal anatomical observations are shown in Table I. Images of several types of injuries are shown in Fig. 3. In Table I, column 2, the pooled control rate, identifies the percent injury for a given effect within the set of 73 control fish used over the four trials. Pooling of these data over the four trials is warranted based on a chi-square (χ^2) test of homogeneity ($p = 0.78$).

Column 3 of Table I, pooled injury, identifies the percent injury based on the pooling of the 20 unique cage ranges sampled over the four trials. Column 4 provides the injury rate SD that incorporates treatment sample size (209), control sample size (73), and any non-zero control injury rates, based on Ricker (1975, p. 123). The p-values for a χ^2 test of homogeneity over the range for given injury are identified in column 5. The p-values for ruptured swim bladder, kidney rupture, burst capillaries, and ruptured reproductive

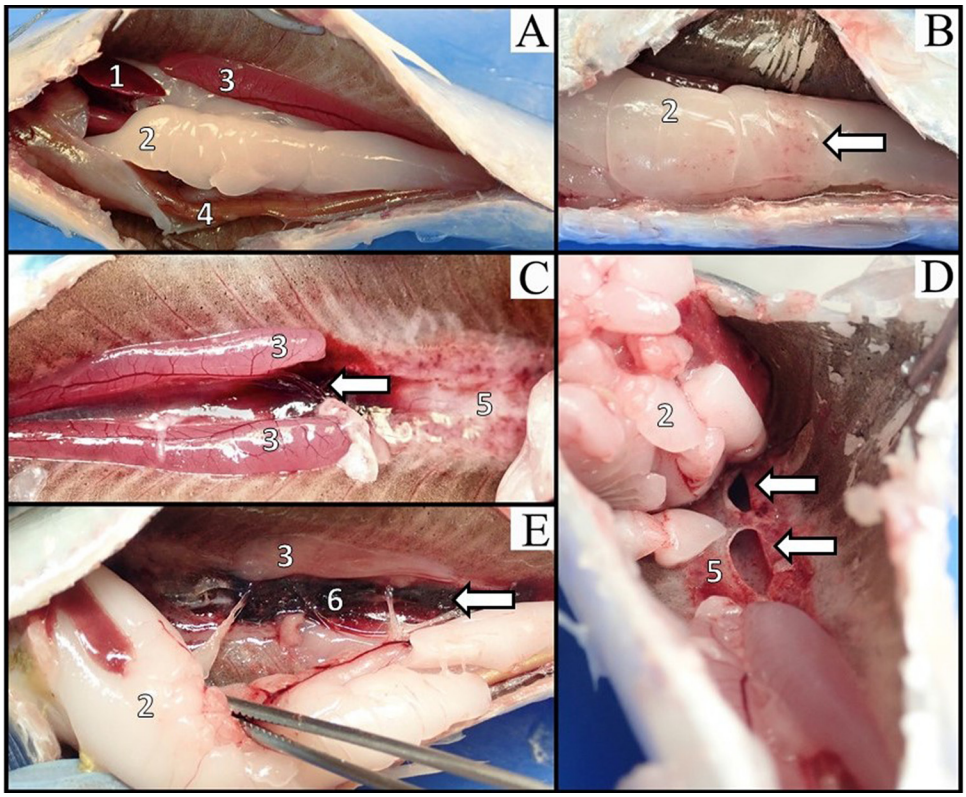

FIG. 3. (Color online) Photographs of internal dissections of Pacific sardines. Numbers indicate the following organs/tissue: (1) liver, (2) fat, (3) gonads, (4) intestine, (5) swim bladder, and (6) kidney. White arrows indicate internal injuries that are statistically different between control and experimental animals. Views are from the ventral side of each animal. (A) Fat from a control fish visible upon opening the body cavity, ventral to the gut; (B) fat hematoma (animal 121 m from explosion); (C) reproductive blood vessel rupture (animal 182 m from explosion); (D) swim bladder rupture (animal 121 m from explosion); (E) kidney rupture visible after removal of swim bladder (animal 30 m from explosion). All fish were of similar size.

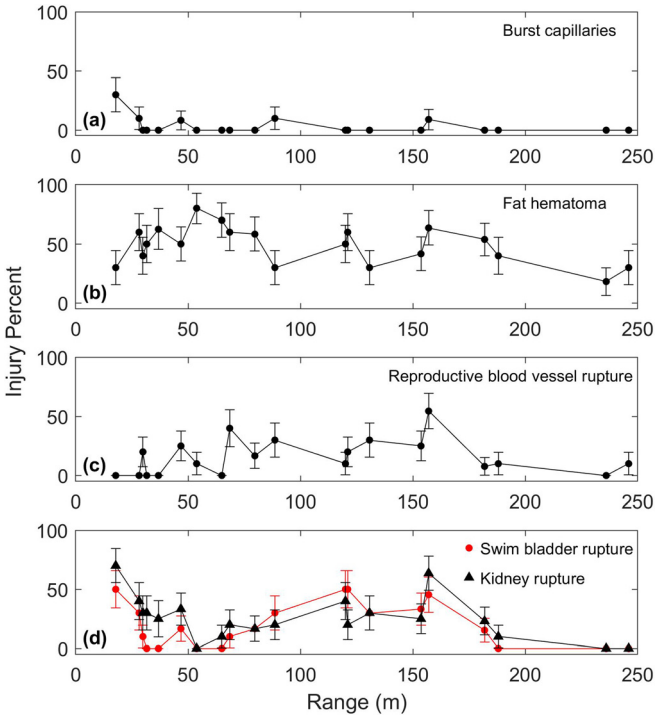

FIG. 4. (Color online) Percent injury for each cage according to their distance from the explosion over the four trials. Data are only shown for injuries that are statistically different from controls (Table I). Error bars represent ± one SD based on specific pooled control rate (Table I) and number of fish in given cage using Ricker (1975). See text for further explanation.

blood vessel are less than 0.05, indicating a rejection of hypothesis that injury is independent of range.

Finally, column 6 provides a single measure of overall injury significance, in the form of the p-value for χ^2 test of H_o: non-injury rate is independent of exposure (or non-injury rate of controls not statistically different from exposed fish). As a reminder, the exposed injury rate used in this analysis is based on the pooling of all 209 exposed fish over the 20 cage ranges, such pooling will tend to increase the p-value for this test. Thus any p-value less than 0.05 is a strong indicator that the injury rate is significant. Similarly, p-values greater than 0.05, while in combination with that injury being statistically homogeneous in range, is an indicator that the injury is not significant. Some exceptions to this classification are identified in Table I.

Results show five injuries that were statistically significant plotted as a function of range in Fig. 4. Burst capillaries are included in this set despite this injury having a relatively low pooled injury rate (column 3, Table I). However, in this case, pooling is not supported ($p = 0.03$, column 5, Table I), and the p-value for injury significance falls below 0.01 upon assessment of the data observed within 50 m of the source [see Fig. 4(a)].

In contrast, fat hematoma [Fig. 4(b)] and reproductive blood vessel ruptures [Fig. 4(c)] were found in many fish at various distances. Indeed, fat hematoma was found in all experimental animals at all distances, but the degree of hematoma, and the variety of location in fat located in different regions of the internal body cavity, makes it hard to correlate with swim bladder motion or any other physical or physiological effect. Findings for reproductive blood vessel ruptures may be related to the impact of swim bladder motions because the blood vessel is located directly ventral to the swim bladder [Fig. 4(e)].

Two significant injuries that are likely to result in eventual mortality, swim bladder rupture and kidney rupture (Stephenson *et al.*, 2010; Halvorsen *et al.*, 2011), are highly correlated with one another (correlation coefficient = 0.71) and so they are plotted together [Fig. 4(d)]. However, neither injury relates simply to the range from the source, nor to the signal level as expressed by peak pressure (Fig. 5). An exception, however, appears to be for ranges less than about 50 m, for which injury rate for rupture of both kidney and swim bladder generally decreases monotonically as range increases [Fig. 4(d)], or decreasing peak pressure (Fig. 5). However, beyond about 50 m, the injury rate increases again reaching a maximum between 100 and 150 m. This effect is examined further in Sec. IV.

B. Acoustic results

Figure 6 provides an overview of acoustic results with respect to range for peak pressure and sound exposure level (SEL) [Fig. 6(a)] and for pressure impulse based on the same data [Fig. 6(b)]. The data are those obtained at each of the exposure test cages. While these data can be expressed in alternate ways, the results in Fig. 6 focus on measures of the acoustic field that might be anticipated to correlate with injuries observed during the experiment.

Thus, with $p(t)$ representing the time series of pressure at any given range, then peak pressure is the maximum of $|p(t)|$ expressed in dB re 1 μPa and SEL is the time integral of $p^2(t)$ expressed in dB re 1 μPa^2-s. These quantities [Fig. 6(a)] decay monotonically with increasing range from the explosive source, as expected, and are furthermore well-described by an empirical equation based on scaled range (Soloway and Dahl, 2014) for which a TNT equivalent weight of 4.66 kg was used (dashed, gray line). The pressure impulse [Fig. 6(b)] decays in the same manner. Here, the cumulative integral of $p(t)$ over time is first computed, and the maximum value is taken as the specific measure of pressure impulse.

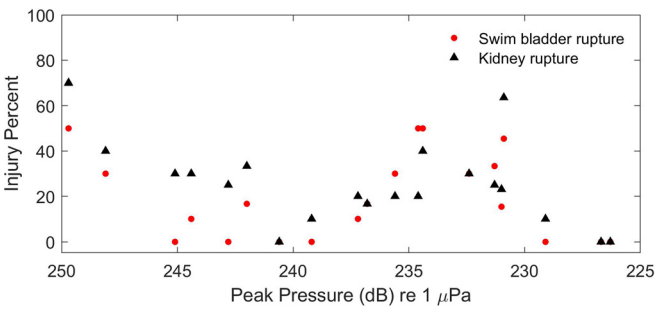

FIG. 5. (Color online) Pattern of percent injury for swim bladder rupture and kidney rupture originally shown in Fig. 4(d) as function of range displayed but here as a function of peak pressure. [Note error bars not shown to emphasize pattern but they are identical to those in Fig. 4(d).]

https://doi.org/10.1121/10.0001064

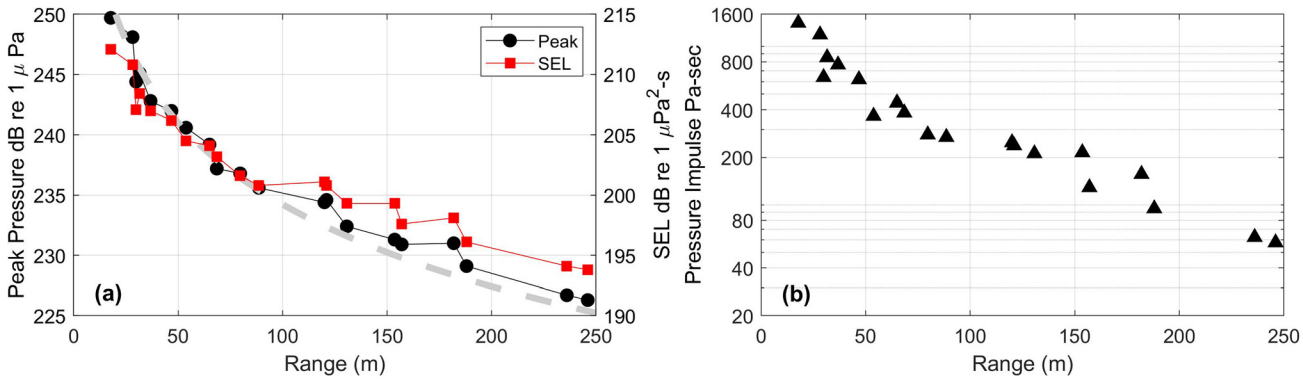

FIG. 6. (Color online) (a) Peak pressure and SEL for all 20 cages as a function of range from the explosive source over the four trials. Dashed-gray line is scaled-range based empirical predication of peak pressure. (b) Pressure impulse from the same data.

IV. DISCUSSION

Results from this study, while limited to a single species and environment, provide new and important insight into potential physical effects of sound from explosions on fishes in open water. The results demonstrate that damage to Pacific sardines exposed within 50 m of the source decreases with increasing range. However, the results also lead to the suggestion that some effects do not necessarily support the expected dose/response relationship between increasing distance (greater than 50 m) and decreasing effect. It is possible that future analyses might demonstrate such a relationship with other species and/or other acoustic conditions.

A. Physical effects

Twelve potential effects were investigated. These were selected based on earlier studies using another impulsive source—pile driving (e.g., Stephenson *et al.*, 2010; Halvorsen *et al.*, 2011; Halvorsen *et al.*, 2012b). As demonstrated in Table I, 7 of the 12 potential effects were either not observed throughout the experiment or did not differ significantly from controls at any distance from the explosion. The remaining five effects, burst capillaries, fat hematoma, reproductive blood vessel rupture, swim bladder rupture, and kidney rupture, were significantly different from controls (alpha = 0.05), as shown in Table I and Fig. 4. Thus, data suggest that these were injuries that could be attributed to exposure to the explosion.

It is interesting, but not easily explained, that some tissues, such as the stomach and gut, located near the swim bladder did not show any damage in the study, whereas such damage occurred in the laboratory study of impulsive pile driving (e.g., Halvorsen *et al.*, 2012a; Halvorsen *et al.*, 2012b) for which repetitive exposure of impulsive sound was simulated. While the reason for the differences in findings are not clear, there are several possibilities, including signal level and impulse characteristics such as rise time. It is also possible that more damage on tissue distant from the swim bladder, as the stomach and gut, occurs when there is repetitive exposure, as in the pile driving studies, but not when there is a single exposure, as in the current study.

The proportion of burst capillaries [Fig. 4(a)] was significantly higher within approximately 20 m from the explosion than in the controls (closest cage vs controls $p = 0.01$). The burst capillaries were generally noted in the body wall and therefore are not in direct contact with the swim bladder. Thus, it might be plausible to assume that this injury did not result from displacement of the swim bladder walls. While the cause for the burst capillaries is not clear, this is something worth examining in future studies.

Pacific sardines have a prominent blood vessel that traverses the ventral surface of the swim bladder and then splits and runs to the bilateral reproductive organs. Considerable damage occurred to this reproductive blood vessel, although the proportion of fish with this injury [Fig. 4(c)] was lower at the closest ranges. For ranges greater than about 50 m, the degree of this injury correlates well with rates of swim bladder and kidney rupture [Fig. 4(d)]. One explanation as to why this injury was not more frequently observed within 50 m is that the considerable damage to the nearby swim bladder obscured observation of this injury in some animals.

Fat hematoma was observed both in the large adipose deposits in the body cavity as well as on fatty connective tissue around the swim bladder. As shown in Fig. 4(b), fat hematoma was seen in fish exposed at every distance (Table I: between treatment heterogeneity $p = 0.394$). The presence of fat hematoma over all distances at which fish were exposed means that, at least at this time, we cannot establish an onset of injury based on the ranges tested in this study. Moreover, the physiological significance of fat hematoma is not clear at this time. We speculate that large deposits of fat in the experimental subjects may be the result of excess feeding and may not be present in wild Pacific sardines, which in turn could reduce the prevalence of this injury in the wild.

Perhaps the most significant finding is for the swim bladder and kidney. While the initial hypothesis in this study was that results would show a decrease in effects at increasing distance from the source, this was not the case for these organs. Instead, results show that both organs had considerable injury in fish exposed within approximately 50 m of the source in this study. Fewer injuries were observed between about 50 and 125 m, as might be predicted from a close relationship between received signal level and damage.

However, results also showed a second region of extensive injury to the swim bladder and kidney from approximately 125 to 150 m, while beyond that distance, and between 200 and 250 m, the level of swim bladder and kidney rupture decreased to zero. In the case of these injuries, the non-monotonic pattern of injury rate evident between 125 and 150 m is a notable result of this study. The proposed mechanisms for this pattern are discussed below.

B. Properties of the underwater acoustic waveguide and detailed inspection of waveforms incident on the caged fish

In previous studies of the effects of explosives and impulse-like anthropogenic sounds on fishes, peak pressure and pressure impulse (Yelverton *et al.*, 1991; Govoni *et al.*, 2003; Govoni *et al.*, 2008), and SEL (e.g., Casper *et al.*, 2012; Halvorsen *et al.*, 2012a) were used as measures of dosage for proximate exposures. Thus, it was anticipated that injury observations in this study (Fig. 5) would show a similar trend with blast strength or distance that mirrors the acoustic data (Fig. 6). However, results [Fig. 4(d)] show that the probability of the major physical impacts (kidney or swim bladder rupture) is high within 20 to 30 m of the source, decreases to a low in the 50 to 70 m range, and then increases again between 120 and 150 m, before declining beyond about 150 m. Thus, while these results do not correlate directly with either peak sound level or SEL (at least beyond about 30 m), a plausible explanation for the pattern of injury with range in Fig. 4(d) is related to properties of an underwater acoustic waveguide that govern the experiment.

The averaged sound speed conditions [Fig. 7(a)] indicated a mild downward refracting sound speed profile owing to a thermocline, and five eigenrays are computed [Fig. 7(b)] using ray theory connecting the source at depth 10.5 m to a cage at depth 10.9 m, range 154 m, representing the dominant contribution at this range. The influence of refraction is best seen in the direct path (1) showing slight downward refraction at 154 m. Other dominant paths are the bottom reflected (2), surface reflected (3), and two multiple surface/bottom reflected paths (4).

For the most part, the first three paths carry the majority of the energy from the explosive source, with the influence of bottom reflection on path 2 changing over range depending on the bottom grazing angle θ, which, for this example, is about 7°. The effect of reflection from the seabed at angle θ is assessed by way of the plane wave reflection coefficient, for which the magnitude and phase is displayed in Fig. 7(c). Here, the computation is based on a sediment sound speed of 1670 m/s, sediment density of 1800 kg/m^3, and sediment attenuation of 0.5 dB/λ, values that are within the ranges

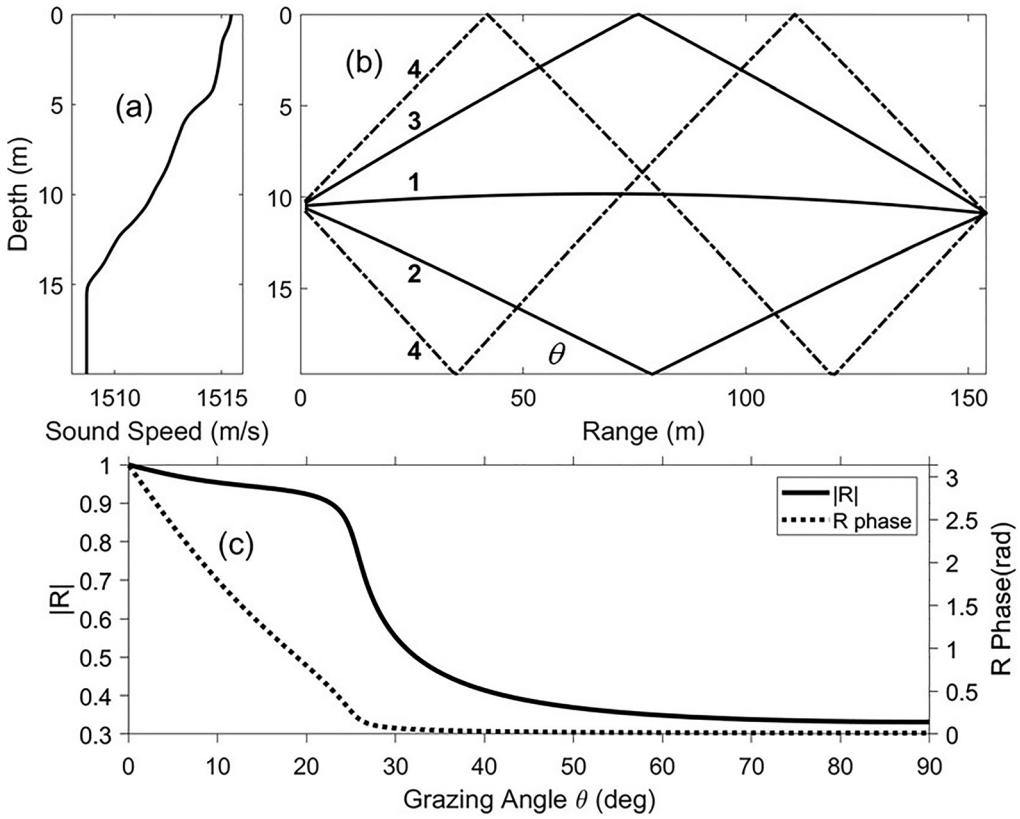

FIG. 7. (a) Sound speed versus depth averaged over the four trials. (b) Ray paths for dominant eigenrays connecting source at depth 10.5 m to receiver at depth 10.9 m and range 154 m, computed using ray theory and the sound speed profile shown in (a). Paths shown by solid lines are of higher amplitude relative to paths shown by dashed lines. Integers correspond to the ray paths as follows: 1, direct path; 2, bottom reflection; 3, surface reflection; and 4 represents two multiple surface/bottom reflections. (c) Magnitude (solid line) and phase (dotted line) of the plane wave reflection coefficient based on the nominal descriptors for a sandy seabed that characterizes the area. See text for detailed explanation.

https://doi.org/10.1121/10.0001064

of observations made from sandy sediments (Yang and Tang, 2017).

Alternate descriptors for the seabed are also possible, but the basic properties displayed in Fig. 7(c) will not change significantly, and in particular, the critical angle delineating the angle below which there is near-total reflection is near 21°. Thus, for the example, for a range of 154 m, the magnitude of the reflection coefficient $|R|$ for the bottom reflected path will be nearly 1, with the reflection coefficient having a substantial phase angle. Some implications of this phase are discussed further in the Appendix.

Figure 8 shows pressure waveforms measured at 28, 68.5, and 154 m from the source detonation. The full measurement bandwidth (1 MHz) version is shown by a thin black line and a low-pass (5 kHz) version by a thick gray line. Note that the 7-ms period of each graph contains the primary arrival structure and energy. Beyond this 7-ms time period, a first, second, and in some cases a third, bubble pulse can be observed at successive delays of about 250 ms, as would be notionally predicted for an explosive charge at this depth and weight (Chapman, 1985).

At 28 m [Fig. 8(a)], the average of the swim bladder and kidney injury rate is 35% [see Fig. 4(d)], and the maximum observed peak pressure and SEL are 247 dB re 1 μPa and 208 dB re1 μPa^2-s, respectively. The direct path (1) and bottom-reflected path (2) are separated by about 4 ms, with amplitude of path 2 reduced to about 40% compared with path 1, which is nominally consistent with the magnitude of the reflection coefficient [Fig. 7(c)] evaluated at grazing angle 35°. Approximately 1-ms later, the sea surface-reflected path (3) arrives and abruptly reduces the pressure. Referring to the full band version, the sequence of sharp spikes at (3), the first of which is negative, is assumed to identify the leading edge of the surface reflected pulse before the onset of cavitation (Wentzell *et al.*, 1969). The smoothed (5 kHz) version of the data shows the waveform reaching a negative pressure of about −100 kPa.

At 68.5 m [Fig. 8(b)], the average of the swim bladder and kidney injury rate falls to 15%, and the maximum observed peak pressure and SEL are 238 dB re 1 μPa and 202 dB re 1 μPa^2-s, respectively. The sequence of arrivals 1-2-3 is compressed because of the longer range, so paths 1

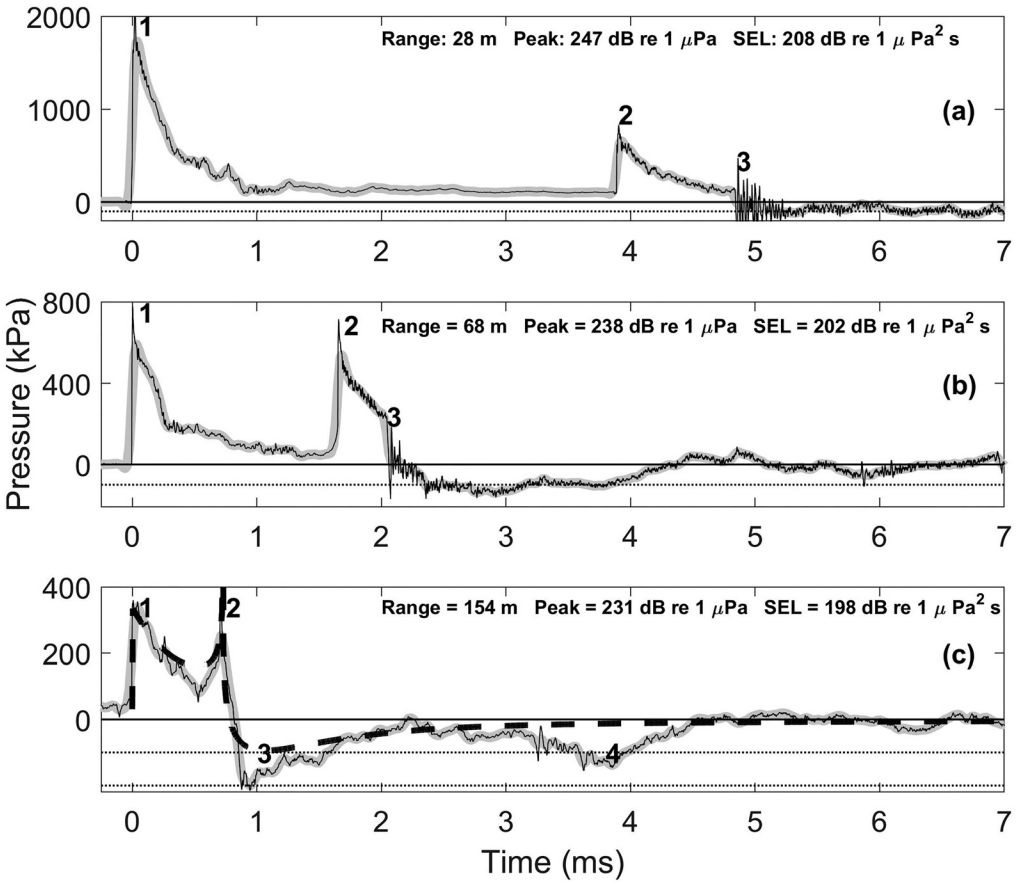

FIG. 8. (a) Time series of peak pressure in kPa measured at range 28 m from the source. The thin black line is original data at 1 MHz bandwidth while thick gray line is a low-pass (5 kHz) version. The numbers 1, 2, 3 identify arrivals of the direct path, bottom reflected path, and sea surface reflected path, respectively [see Fig. 7(b)]. Cavitation onset from the sea surface is indicated by the highly oscillatory behavior seen in the full bandwidth data (also see text), which stabilizes to approximately −100 kPa in the low-pass result; the black solid and dotted lines identify 0 and −100 kPa reference lines, respectively. (b) Same as (a) but measured at range of 68 m. (c) Same as (a) but measured at range of 154 m with a third reference line, −200 kPa, shown and an additional number, 4, identifies two multiple surface, bottom reflected arrivals that arrive at nearly the same time. Black, dashed line represents model for direct and bottom reflected paths as discussed in the Appendix.

and 2 are now closer in amplitude as might be anticipated by the grazing angle of ~18°. Arrival of path 3 about 0.5 ms after arrival of the bottom reflected path 2 [predicted by ray theory using the sound speed profile of Fig. 7(a)] represents an excellent example of the cavitation surface cut-off effect (as in Wentzell *et al.*, 1969).

Finally, at 154 m [Fig. 8(c)], the average of the swim bladder and kidney injury rate has risen to 30% though the peak pressure and SEL have decayed and are 231 dB re 1 μPa and 198 dB re 1 μPa^2-s, respectively. The sequence of arrivals 1-2-3 is further compressed and, importantly, negative pressure has now reached about −200 kPa, falling to the value in a distinctly more rapid manner than observed at the other two ranges.

A simplified model curve (dashed line) is also shown, but it is limited to the portion of the explosive waveform associated with paths 1 and 2. Derivation of this line is given in the Appendix, but the key point is that the bottom reflected path, by itself and without contribution from the negative reflection from the sea surface, leads to substantial negative pressure of about −100 kPa, to which the contribution from the sea surface is expected to push this further toward −200 kPa.

Not all waveforms associated with the four tests conducted at five ranges display the above properties of negative pressure, insofar as (i) low-pressure point and (ii) rate of pressure change, versus range as clearly as the examples in Fig. 8. However, the examples in Fig. 8 do capture the sense of the acoustic data, and show a roughly similar relation with other data within the approximate range interval 100–175 m, which aligns with the increased injury rate for both the strongly correlated ruptured swim bladder and ruptured kidney injuries [Fig. 4(d)].

Finally, it is important to reiterate that these specific acoustic waveguide results depend on bottom properties similar to those in this study and, to some extent, to a similar water depth. While the same general waveguide effects may be seen in other environments, the results reported here cannot be extrapolated to other depths and bottoms without a fuller understanding of the effects in a broader range of environments.

C. Mechanisms of physical effects

There is growing agreement in the literature that much of the internal physical damage from exposure to impulsive acoustic stimuli is a result of the interactions between the gas-filled swim bladder in the abdominal cavity and the nearby (and often contacted) soft tissues such as the kidney (e.g., Goertner *et al.*, 1994; Carlson, 2012; Halvorsen *et al.*, 2012a; Carlson *et al.*, 2019). This observation is supported by findings that physical effects from exposure to impulsive pile driving, similar to those seen in this study, were found in fishes with a swim bladder, and not in a species without a swim bladder (Halvorsen *et al.*, 2012a). Similarly, a study of injuries to fishes without a swim bladder that were exposed to an explosion also showed fewer physical effects compared to fishes with swim bladders (Goertner *et al.*, 1994). Further supporting this argument, it is important to note that the greatest injury in the current study was to the swim bladder as well as to the kidney and reproductive blood vessel, which lie dorsal to and ventral to the surface of the swim bladder, respectively.

Following from the idea of swim bladder involvement, the acoustic analysis leads to the suggestion that, at a range of 154 m (this being a specific example), the greater rate of pressure change and deeper low-pressure point during the decompression phase are linked to swim bladder expansion damage and rupture. This includes damage to immediately neighboring organs as manifested by the kidney data that are highly correlated with the swim bladder data. This is the proposed cause of the observed higher injury rate at 154 m despite the higher peak pressures observed at 68 m, and has been suggested by earlier models of swim bladder related injury (Goertner, 1978; Wiley *et al.*, 1981).

To see how this can happen, the acoustic pressure data of Fig. 8 is converted to absolute pressure by adding one atmosphere (101.3 kPa) plus the depth-dependent hydrostatic pressure (105.5 kPa based on measurement depth of 10.5 m). Thus, we assume a static pressure P_A of 206.8 kPa, and the low pressure the fish were subject to, or minimum decompression pressure P_D, is estimated to be 106, 81, and 7 kPa at respective ranges 28, 68, and 154 m (Fig. 8). These estimates were based on the smoothed, low-pass version of the data (Fig. 8) upon adding P_A.

For a constant temperature, Boyle's law puts the ratio of swim bladder volume at maximum decompression V_{Dmax} compared with that at the acclimation (or static) pressure V_A equal to ~2, 2.5, and ~30 for the same increasing range set, and it can be assumed that swim bladder tissues (and any other air-filled tissues) have undergone considerably more strain at range 154 m. Note that the issue of swim bladder tissue compliance is beyond the scope of this study, and thus we assume that pressure reduction has produced a volume expansion that is instead bounded by Boyle's law. For example, Stoyek *et al.* (2011), in a study of tissue compliance, showed that Boyle's law predicted well the volume changes in the swim bladder of zebrafish (*Danio rerio*) during compression but had an upper bound during expansion.

That being said, it is interesting that Brown *et al.* (2012) also determined that the main factor associated with the mortal injury of juvenile Chinook salmon during their study on simulated turbine passage was the ratio between the acclimation pressure and the lowest exposure pressure, this being the same ratio as defined above.

A possible related explanatory variable is formed upon combining the rate of pressure change and minimum decompression pressures as follows. We take the time derivative of Boyle's law in the form

$$V_D(t) = V_A P_A / P_D(t), \tag{1}$$

where the decompression volume $V_D(t)$ and pressure $P_D(t)$ vary with time during the decompression phase, which gives

https://doi.org/10.1121/10.0001064

$$\dot{V}_D(t)/V_A = -P_A\dot{P}_D(t)/P_D^2(t), \quad (2)$$

where dot notation for time differentiation is used. Equation (2) describes a volumetric strain rate, or fractional increase in volume per unit time, with dimension 1/s. A means to obtain consistent and robust estimates of both $\dot{P}_D(t)$ and $P_D^2(t)$ from all the raw acoustic data remains under study; however, inspection of smoothed waveforms in (Fig. 8) immediately suggests that for range 154 m [Fig. 8(c)], there is clearly a larger value of $\dot{P}_D(t)$ based on the slope of the pressure decay corresponding to the arrivals of paths 2 and 3, and a smaller value of $P_D^2(t)$, leading to much higher estimate of volumetric strain rate.

A mechanism for damage to the swim bladder or other air-filled voids cannot be attributed solely to high volumetric strain rate nor volume expansion at maximum decompression. For example, this effect would not explain our necropsy observations for ranges less than about 50 m [Fig. 4(d)], a range interval where the three acoustic metrics (Fig. 5) appear to show correlation with injury and are thus more valid explanatory variables. Furthermore, Wiley *et al.* (1981) discuss a mechanism for swim bladder oscillations imparted by the positive-going shockwave. A degree of oscillatory swim bladder response is expected because of the impulsive loading, which could contribute to the effects found at close range. However, in the current study, the continued decay of pressure impulse with range [Fig. 6(b)] is at variance with the injury data once the range exceeds about 50 m, and consideration of rarefaction effects on swim bladder expansion may be more relevant to injury potential.

D. Study species

Teleost fishes use their swim bladder for buoyancy and for maintaining position in the water column with minimal expenditure of energy (e.g., Helfman *et al.*, 2009). Pacific sardines (and all Clupeiformes) are physostomous fishes and periodically go to the surface and gulp air, which they move from the esophagus to the swim bladder via a small pneumatic duct. In the current study, it was not possible to know the ultimate fill status of the swim bladder after the acclimatization period at the experimental depth. The significance of this is that the response of the swim bladder to acoustic stimulation when the fish is at the experimental depth may differ depending on whether it is full, with fully expanded walls, or not. For example, if the walls are not fully expanded, they are less likely to impact surrounding tissues when exposed to an impulsive sound, resulting in less potential damage to surrounding tissues (Halvorsen *et al.*, 2012a).

At the same time, it should be noted that all of the fish cages were observed using an ROV while they were at depth prior to the explosion. The majority of fish were schooling in mid-cage (Fig. 1) and did not appear to show any obvious signs of buoyancy issues (i.e., exerting excess energy to maintain their depth). Thus, it is possible to hypothesize that the swim bladders in the fish was normally inflated for the experimental depth.

The Pacific sardine is representative of what is one of the most commercially important group of fishes in the world, the Clupeiformes (herrings, sardines, and relatives). While it is tempting to extrapolate from this species to other clupeids and fishes in other unrelated taxa, this needs to be done with utmost caution because is not known whether the anatomical and physiological differences between Pacific sardines and fishes in other taxa would also affect how they respond to underwater explosions. While recent work on effects of pile driving sounds shows there is some similarity in effects between species that are morphologically distinct, they also suggest caution in trying to extrapolate from a single species (Halvorsen *et al.*, 2012a; Casper *et al.*, 2017), particularly until there are comparable data to those presented here for a number of anatomically distinct fish species. Such caution also derives from similar concerns about extrapolation between species made in the most recent guidelines for potential effects of sound on fishes (Popper *et al.*, 2014; Popper and Hawkins, 2019).

V. CONCLUSIONS

While the results presented here are for a single species at a single depth, they still provide important insight into potential effects on fishes exposed to sound from explosions. The results also raise important issues with how effects of these sounds should be analyzed in the future. A detailed understanding of the acoustic field as related to water depth, bottom characteristics, and other aspects of propagation are clearly critical.

It is also important to understand that results should only be extrapolated to other species with the greatest caution. Indeed, this study should be thought of as only the first of a number that are needed in order to understand the potential effects of sounds from underwater explosions on fishes. Important variables to investigate in future studies are, among others, different species/morphologies, depth of exposure, different depths of water, and different bottom types. Furthermore, results reported here are likely related to the specific size of the explosion, source and receiver geometry, and other aspects of the acoustic environment.

Moreover, while it is suggested that swim bladder rupture and kidney rupture are mortal injuries, this is still conjecture since animals were euthanized on return to the surface. Thus, it would be important to conduct survival studies where fish are not euthanized and monitored for some period of time after exposure. The only studies which examined survival showed that several species of fish recover from exposure to intense impulsive pile driving sounds (Casper *et al.*, 2012; Casper *et al.*, 2013), while recognizing that subjects were fed and not exposed to predators or adverse environmental conditions during recovery.

ACKNOWLEDGMENTS

This study was presented at the July 2019 meeting on Effects of Noise on Aquatic Life in Den Haag, the Netherlands. This project could not have been completed

without the assistance from Alyssa Accomando, Dana Schrimpf, and Cameron Martin, and the overwhelming support of several other NIWC Pacific teams: facilities (Depot), veterinary technicians, and the ROV team. The authors thank EOD Mobile Unit Three Detachment Southwest, the U.S. Third Fleet, and the U.S. Pacific Fleet for enabling a safe and successful field effort. Our fish were collected and cared for with the help of Kathy Swiney, John Hyde, Nick Wegner, and Scott Mau at Southwest Fisheries Science Center. The investigators also appreciate valuable discussions and guidance from Dr. John Skalski and Dr. Rich Townsend of the University of Washington relating to statistical analysis. We also thank Dr. Anthony D. Hawkins and Dr. Christopher Platt for critical review and insightful comments on an earlier version of the paper. The study was supported by the Living Marine Resources (LMR) program of the U.S. Navy and we are most grateful for their financial support. The views expressed in this publication reflect the results of research conducted by the author(s) and do not necessarily reflect the official policy or position of the Department of the Navy, Department of Defense, nor the U.S. Government. Some of the authors are employees of the U.S. Government. This work was prepared as part of their official duties. Title 17 U.S.C. §105 provides that "Copyright protection under this title is not available for any work of the United States Government." Title 17 U.S.C. §101 defines a U.S. Government work as a work prepared by an employee of the U.S. Government as part of that person's official duties.

APPENDIX: SIMPLIFIED MODEL FOR PORTION OF THE EXPLOSIVE WAVEFORM INCIDENT ON THE CAGED FISH

A simplified model for the portion of the explosive waveform associated with paths 1 and 2 in Fig. 8(c) is outlined in this appendix. The goal is to capture the primary physics that can assist interpretation of the data and, in particular, show how bottom reflection can amplify negative pressure possibly leading to greater injury.

The analysis applies equations from Chapman (1985), derived from scaled range theory, hereafter referred to as C85, that are governed by range from the source and W, or TNT equivalent weight (4.66 kg). That scaled range applies to this study can be confirmed through inspection of results in Fig. 6(a).

For path 1, or the direct path, the slight curvature caused by refraction is ignored and assume a straight path, putting range $r_1 = 154$ m. The direct path waveform $P_{DP}(t)$ is modeled as an exponential of the form

$$P_{DP}(t) = \hat{P}_{DP} e^{-t/\tau_{DP}}, \tag{A1}$$

where $\hat{P}_{DP}$ is the shock impulse peak pressure amplitude based on C85 Eq. (1), and τ_{DP} is the time constant based on C85 Eq. (12). Note that time $t = 0$ in the Eq. (A1) is referenced to the onset of the direct path as observed at range 154 m, which we take as r_1/c, where c is a depth-averaged sound speed (1513 m/s).

Path 2, due to bottom reflection, is a most interesting feature of this study. As a first step, the peak pressure $\hat{P}_{BP}$ and time scale τ_{BP} for a bottom-reflected path are also modeled as in Eq. (A1), where, in this case, the range is set equal to the total extent of path 2, call it r_2, again taken as a straight ray path determined by the geometry.

The bottom reflected pulse is further modified by the reflection coefficient R. It is emphasized that, in line with the simplicity of this model, R is derived from the *plane wave* reflection coefficient [Fig. 7(c)] from a sediment half-space, which is independent of frequency. Referring now to Fig. 7(c), the bottom grazing angle θ for path 2 is $\sim 7°$, which puts $|R| \sim 0.94$ (about 0.5 dB of reflection loss) with phase equal to about 2 radians. The small grazing angle, well inside the critical angle of 21°, provides some additional justification for using the plane wave reflection coefficient. For closer ranges, and in particular ranges in the vicinity of the critical angle, a more complex spherical wave reflection formulation (Westwood, 1989) would likely be necessary.

Given the pressure field of high bandwidth incident on the seabed, it is expected that the substantial phase angle will distort the bottom-reflected pulse (Cron and Nuttall, 1965). Let $R(\theta)$ be the complex reflection coefficient evaluated at $\theta = 7°$ with both magnitude and phase given in the preceding paragraph; then to embody the effects of complex-valued reflection coefficient in the bottom reflected path, we employ a Hilbert transform as follows:

$$P_{BP}(t) = Re\left\{H(\hat{P}_{BP} e^{-t/\tau_{BP}})\, R(\theta)\right\}, \tag{A2}$$

where H represents the Hilbert transform and time $t = 0$ is referenced to the onset of the bottom-reflected path equal to r_2/c.

The two contributions Eqs. (A1) and (A2) are added, with the latter delayed by time r_2/c. This gives the model curve shown in Fig. 8(c), which captures the sense of the combination of the direct and bottom reflected arrival. It is seen that bottom reflection at this range, by itself, produces a distorted pulse with sharper peak, a faster decay towards negative pressure, and substantial negative pressure to which additional negative pressure originating from the sea surface will be added.

Note that similar but more detailed modeling of the explosive waveform limited to short ranges and without boundary reflections is found in Wilson *et al.* (2019). Key differences between this study and that of Wilson *et al.* are that here the bubble pulse contribution is not included for the reason discussed in the context of Fig. 8, and for further simplicity a single time scale τ_{DP} is used.

[1]For more information, see www.hstteis.com.

Brown, R. S., Carlson, T. J., Gingerich, A. J., Stephenson, J. R., Pflugrath, B. D., Welch, A. E., Langeslay, M. J., Ahmann, M. L., Johnson, R. L.,

Skalski, J. R., Seaburg, A. G., and Townsend, R. L. (**2012**). "Quantifying mortal injury of juvenile Chinook salmon exposed to simulated hydro-turbine passage," Trans. Am. Fish. Soc. **141**, 147–157.
Carlson, T. J. (**2012**). "Barotrauma in fish and barotrauma metrics," in *The Effects of Noise on Aquatic Life*, edited by A. N. Popper and A. D. Hawkins (Springer, New York), pp. 229–233.
Carlson, T. J., Johnson, G. E., Skalski, J. R., and Woodley, C. M. (**2019**). "Estimating the take of migrating adult chum salmon (*Oncorhynchus keta*) caused by confined underwater rock blasting," Environ. Impact Assess. Rev. **77**, 85–92.
Carroll, A. G., Przeslawski, R., Duncan, A., Gunning, M., and Bruce, B. (**2017**). "A critical review of the potential impacts of marine seismic surveys on fish and invertebrates," Mar. Poll. Bull. **114**, 9–24.
Casper, B. M., Halvorsen, M. B., Carlson, T. J., and Popper, A. N. (**2017**). "Onset of barotrauma injuries related to number of pile driving strike exposures in hybrid striped bass," J. Acoust. Soc. Am. **141**, 4380–4387.
Casper, B. M., Halvorsen, M. B., Matthews, F., Carlson, T. J., and Popper, A. N. (**2013**). "Recovery of barotrauma injuries resulting from exposure to pile driving sound in two sizes of hybrid striped bass," PLoS One **8**, e73844.
Casper, B. M., Popper, A. N., Matthews, F., Carlson, T. J., and Halvorsen, M. B. (**2012**). "Recovery of barotrauma injuries in Chinook salmon, *Oncorhynchus tshawytscha* from exposure to pile driving sound," PLoS One **7**, e39593.
Chapman, N. R. (**1985**). "Measurement of the waveform parameters of shallow explosive charges," J. Acoust. Soc. Am. **78**, 672–681.
Coker, C. M., and Hollis, E. H. (**1950**). "Fish mortality caused by a series of heavy explosions in Chesapeake Bay," J. Wildlife Manage. **14**, 435–445.
Cron, B. F., and Nuttall, A. H. (**1965**). "Phase distortion of a pulse caused by bottom reflection," J. Acoust. Soc. Am. **37**, 486–492.
Gaspin, J. B. (**1975**). "Experimental investigations of the effects of underwater explosions on swimbladder fish, I: 1973 Chesapeake Bay tests," Naval Surface Weapons Center Report NSWC/WOL/TR (NSWC, Washington Naval Yard, Washington, DC), pp. 75–58.
Goertner, J. F. (**1978**). "Dynamical model for explosion injury to fish," Naval Surface Weapons Center (NSWC, White Oak Lab, Silver Spring, MD).
Goertner, J. F., Wiley, M. L., Young, G. A., and McDonald, W. W. (**1994**). "Effects of underwater explosions on fish without swimbladders," Naval Surface Weapons Center (NSWC, White Oak Lab, Silver Spring, MD).
Govoni, J. J., Settle, L. R., and M. A., West (**2003**). "Trauma to juvenile pinfish and spot inflicted by submarine detonations," J. Aquatic An. Health **15**, 111–119.
Govoni, J. J., West, M. A., Settle, L., Lynch, R. T., and Greene, M. D. (**2008**). "Effects of underwater explosions on larval fish: Implications for a coastal engineering project," J. Coastal Res. **2**, 228–233.
Halvorsen, M. B., Casper, B. M., Matthews, F., Carlson, T. J., and Popper, A. N. (**2012a**). "Effects of exposure to pile-driving sounds on the lake sturgeon, Nile tilapia and hogchoker," Proc. R. Soc. B **279**, 4705–4714.
Halvorsen, M. B., Casper, B. M., Woodley, C. M., Carlson, T. J., and Popper, A. N. (**2011**). "Hydroacoustic impacts on fish from pile installation," National Cooperative Highway Research Program Research Results Digest 363.
Halvorsen, M. B., Casper, B. M., Woodley, C. M., Carlson, T. J., and Popper, A. N. (**2012b**). "Threshold for onset of injury in Chinook salmon from exposure to impulsive pile driving sounds," PLoS One **7**, e38968.
Hawkins, A. D., and Popper, A. N. (**2018**). "Effects of man-made sound on fishes," in *Effects of Anthropogenic Noise on Animals*, edited by H. Slabbekoorn, R. J. Dooling, A. N. Popper, and R. R. Fay (Springer Nature, New York), pp. 145–177.
Helfman, G., Collette, B. B., Facey, D. E., and Bowen, B. W. (**2009**). *The Diversity of Fishes: Biology, Evolution, and Ecology* (John Wiley & Sons, New York).
Hubbs, C. L., and Rechnitzer, A. B. (**1952**). "Report on experiments designed to determine effects of underwater explosions on fish life," Calif. Fish Game **38**, 333–366, available at https://www.scopus.com/record/display.uri?eid=2-s2.0-0004788584&origin=inward&txGid=be42d0ad30b4365139cb03d9c7437e22.
Linton, T., Landry, A., Jr., Buckner, J., Jr., and Berry, R. (**1985**). "Effects upon selected marine organisms of explosives used for sound production in geophysical exploration," Texas J. Sci. **37**, 341–353, available at http://hdl.handle.net/1969.3/20738.
Miller, D. J., and Lee, R. N. (**1972**). "Guide to the coastal marine fishes of California," California Fish Bulletin Number 157 (State of California Department of Fish and Game, Sacramento, CA).
NMFS (**2018**). "2018 Revisions to: Technical Guidance for Assessing the Effects of Anthropogenic Sound on Marine Mammal Hearing (Version 2.0): Underwater Thresholds for Onset of Permanent and Temporary Threshold Shifts" (US Department of Commerce, Washington, DC), p. 167.
Popper, A. N., Gross, J. A., Carlson, T. J., Skalski, J., Young, J. V., Hawkins, A. D., and Zeddies, D. (**2016**). "Effects of exposure to the sound from seismic airguns on pallid sturgeon and paddlefish," PLoS One **11**, e0159486.
Popper, A. N., and Hawkins, A. D. (**2016**). *The Effects of Noise on Aquatic Life II* (Springer Science+Business Media, New York).
Popper, A. N., and Hawkins, A. D. (**2019**). "An overview of fish bioacoustics and the impacts of anthropogenic sounds on fishes," J. Fish Biol. **94**, 692–713.
Popper, A. N., Hawkins, A. D., Fay, R. R., Mann, D. A., Bartol, S., Carlson, T. J., Coombs, S., Ellison, W. T., Gentry, R. L., Halvorsen, M. B., Lokkeborg, S., Rogers, P. H., Southall, B., Zeddies, D., and Tavolga, W. A. (**2014**). *ASA S3/SC1. 4 TR-2014 Sound Exposure Guidelines for Fishes and Sea Turtles: A Technical Report Prepared by ANSI-Accredited Standards Committee S3/SC1 and Registered with ANSI* (Springer, New York).
Popper, A. N., Hawkins, A. D., and Halvorsen, M. B. (**2019**). *Anthropogenic Sound and Fishes* (Washington State Department of Transportation, Olympia, WA).
Putland, R. L., Montgomery, J. C., and Radford, C. A. (**2019**). "Ecology of fish hearing," J. Fish Biol. **95**, 39–52.
Ricker, W. E. (**1975**). *Computation and Interpretation of Biological Statistics of Fish populations* (Department of the Environment, Fisheries and Marine Service, Ottawa, Canada).
Soloway, A. G., and Dahl, P. H. (**2014**). "Peak sound pressure and sound exposure level from underwater explosions in shallow water," J. Acoust. Soc. Am. **136**, EL218–EL223.
Southall, B. L., Finneran, J. J., Rcichmuth, C., Nachtigall, P. E., Ketten, D. R., Bowles, A. E., Ellison, W. T., Nowacek, D. P., and Tyack, P. L. (**2019**). "Marine mammal noise exposure criteria: Updated scientific recommendations for residual hearing effects," Aquatic Mam. **45**, 125–232.
Stephenson, J. R., Gingerich, A. J., Brown, R. S., Pflugrath, B. D., Deng, Z., Carlson, T. J., Langeslay, M. J., Ahmann, M. L., Johnson, R. L., and Seaburg, A. G. (**2010**). "Assessing barotrauma in neutrally and negatively buoyant juvenile salmonids exposed to simulated hydro-turbine passage using a mobile aquatic barotrauma laboratory," Fish. Res. **106**, 271–278.
Stoyek, M. R., Smith, F. M., and Croll, R. P. (**2011**). "Effects of altered ambient pressure on the volume and distribution of gas within the swimbladder of the adult zebrafish, *Danio rerio*," J. Exp. Biol. **214**, 2962–2972.
Wentzell, R. A., Scott, H. D., and Chapman, R. P. (**1969**). "Cavitation due to shock pulses reflected from the sea surface," J. Acoust. Soc. Am. **46**, 789–794.
Westwood, E. K. (**1989**). "Complex ray methods for acoustic interaction at a fluid–fluid interface," J. Acoust. Soc. Am. **85**, 1872–1884.
Wiley, M. L., Gaspin, J. B., and Goertner, J. F. (**1981**). "Effects of underwater explosions on fish with a dynamical model to predict fishkill," Ocean Sci. Eng. **6**, 223–284.
Wilson, P. S., Knobles, D. P., Dahl, P. H., McNeese, A. R., and Zeh, M. C. (**2019**). "Short-range signatures of explosive sounds in shallow water used for seabed characterization," IEEE J. Oceanic Eng. **45**, 1–12.
Yang, J., and Tang, D. (**2017**). "Direct measurements of sediment sound speed and attenuation in the frequency band of 2–8 kHz at the target and reverberation experiment site," IEEE J. Oceanic Eng. **42**, 1102–1109.
Yelverton, J. T., Richmond, D. R., Hicks, W., Saunders, K., and Fletcher, E. R. (**1991**). "The relationship between fish size and their response to underwater blast," Defense Nuclear Agency, Washington, DC, pp. 91-220.